

Magnetization and static scaling of the high- T_c disordered molecular-based magnet $V(\text{tetracyanoethylene})_x \cdot y(\text{CH}_3\text{CN})$ with $x \sim 1.5$ and $y \sim 2$

P. Zhou and B. G. Morin

Department of Physics, The Ohio State University, Columbus, Ohio 43210-1106

Joel S. Miller*

Science and Engineering Laboratories, Experimental Station E328, du Pont, Wilmington, Delaware 19880-0328

A. J. Epstein

Department of Physics and Department of Chemistry, The Ohio State University, Columbus, Ohio 43210-1106

(Received 16 April 1993)

We report field (H) and temperature (T)-dependent magnetization (M) of a member of the new class of high- T_c molecular-based magnets $V(\text{tetracyanoethylene})_x \cdot y(\text{solvent})$ with T_c in an accessible range (solvent = CH_3CN). The $M(H)$ at low T saturates slowly with increasing H . The random magnetic anisotropy model is applied to study the behavior of this disordered material, yielding values of anisotropy strengths and exchange constant. The results of an equation-of-state and scaling analysis near T_c are given and compared to theoretical results.

Magnetic properties of a new class of molecular-based magnets have been of recent interest,¹⁻⁵ though the magnetic ordering temperature T_c has been confined to less than 10 K. An ~ 50 -fold increase in T_c occurred with the discovery of magnetism at room temperature in the disordered molecular-based $V(\text{TCNE})_x \cdot y(\text{CH}_2\text{Cl}_2)$ ($x \sim 2$, $y \sim 0.5$; $\text{TCNE} \equiv \text{tetracyanoethylene}$).⁶ Its estimated $T_c \sim 400$ K exceeds the decomposition temperature of 350 K. An understanding of the magnetism of this system is important in generating a broad class of molecular-based materials displaying cooperative magnetic behavior at high temperature.

In this work, we report studies of a new related disordered high- T_c molecular-based magnetic compound, $V(\text{TCNE})_x \cdot y(\text{CH}_3\text{CN})$, with T_c in a readily accessible range enabling quantitative study of its critical behavior. The slow saturation of $M(H)$ at low T is shown to be well represented by the random magnetic anisotropy (RMA) model. Detailed application of a RMA theory provides a quantitative link between the magnetization and the limited structural correlation length caused by dilution with spinless CH_3CN . It is suggested from equation of state and static scaling analyses that the RMA gives rise to a strong orientational fluctuation of local magnetization. We conclude that the dominance of RMA effects is due to the structural and substitutional disorder caused by incorporation of spinless solvent. These results extend the success of earlier applications of RMA concepts to site-diluted and amorphous rare-earth and transition-metal materials⁷⁻⁹ to p and d orbital-based spins.

Samples of $V(\text{TCNE})_x \cdot y(\text{CH}_3\text{CN})$ were prepared in a manner similar to the previously reported⁶ $V[\text{TCNE}]_x \cdot y(\text{CH}_2\text{Cl}_2)$. Due to the extreme insolubility of the precipitate and incorporation of the solvent, the concentrations of TCNE and solvent are difficult to control and vary from sample to sample. For the material discussed herein $x \sim 1.5$ and $y \sim 2$ are obtained from elemental analyses. X-ray diffraction shows¹⁰ that structur-

al short-range order ($R_a \sim 10$ Å) is smaller than that for $V(\text{TCNE})_x \cdot y(\text{CH}_2\text{Cl}_2)$ ($R_a \sim 25$ Å). Assuming that V^{II} has three electrons in $3d$ orbitals ($S = \frac{3}{2}$) and TCNE^- has $S = \frac{1}{2}$ with its unpaired electron in an orbital of p_z character at each of the C and N sites, magnetocrystalline anisotropy and single-ion anisotropy should be present for this disordered compound containing non- S -state ions. Randomness in the anisotropy is introduced by dilution of magnetic TCNE^- by nonmagnetic CH_3CN , facilitated by the ability of the $-\text{C} \equiv \text{N}$ groups of CH_3CN to coordinate with the V ions in a manner similar to the $-\text{C} \equiv \text{N}$ of the TCNE anions. The effects of back bonding due to the $\pi-\pi^*$ bonding between V and CN can give rise to a strong irregular ligand field¹¹ dependent on the origin and location of the $-\text{C} \equiv \text{N}$ in this disordered material, while weak electron hopping among V^{2+} and TCNE^- has been suggested to be the primary mechanism for exchange interaction.^{1,6,12,13} The unusual magnetic features of this disordered material reported below are in agreement with application of the RMA model. As available theories of RMA are only valid either at $T=0$ K or near T_c , we first focus on the studies of magnetization at low temperatures, and we then discuss our isothermal M results near T_c .

Most theoretical studies of RMA are based on the Hamiltonian

$$\hat{H} = -J \sum_{i,j} \mathbf{S}_i \cdot \mathbf{S}_j - D_r \sum_i (\hat{n}_i \cdot \mathbf{S}_i)^2 - D_c \sum_i (S_i^z)^2 - g\mu_B \sum_i \mathbf{H} \cdot \mathbf{S}_i,$$

where D_r is a measure of the random uniaxial anisotropy strength, \hat{n}_i is a unit vector corresponding to a random field that points in the direction of local anisotropy, D_c is the strength of the uniform anisotropy, and J is the exchange constant. In the framework of a weak RMA ($D_r/J \ll 1$) real-space model, Chudnovsky and co-workers¹⁴⁻¹⁶ have shown that the magnetic properties at

low temperature ($T \sim 0$ K) are characterized by the correlation function of local anisotropy directions $C(r)$ defined by $C(r)=1$ as $r \rightarrow 0$ and $C(r)=0$ for $r \gg R_a$, relating structural order to magnetic behavior. The approach of M to saturation (M_s) along the direction of an applied field is given by¹⁶

$$M = M_s - \frac{K^2 R_H}{30 A^2} \int_0^\infty dr e^{-r/R_H} r^2 C(r), \quad (1)$$

where $R_H = [A/M_0(H+H_c)]^{1/2}$, $K = D_r/a^3$, $A = zJ/12a$, H_c is the uniaxial (constant) anisotropy field ($\propto D_c$), and a is the mean distance between spin sites (z nearest neighbors). For applied field far from the exchange field, the magnetization obeys three "universal" laws:¹⁵⁻¹⁷ (1) for $(H+H_c) \gg H_{ex}$ (near collinear phase), $M = M_s - (M_s/15)[2K/(H+H_c)]^2$; (2) for $H_s < H+H_c \ll H_{ex}$ [ferromagnet with wandering axis (FWA) phase],

$$M = M_s - B/(H+H_c)^{1/2}, \quad (2)$$

and (3) for $(H+H_c) < H_s$ [correlated spin-glass (CSG) phase], $M = 0$. Here

$$H_{ex} = 2zJa^2M_0/(\pi^2M_sR_a^2), \quad (3)$$

$$B = \frac{\Lambda^2 H_{ex}^{1/2}}{120\pi} \left[\frac{\Omega}{R_a^3} \right], \quad (4)$$

$$\Lambda = \frac{12D_rM_s^{1/2}}{zJ} \left[\frac{R_a}{a} \right]^2, \quad (5)$$

$H_s = H_r^4/H_{ex}^3$, $H_r = 2nD_r\mu_B M_0/M_s^2$ with spin density n , M_0 is the magnitude of \mathbf{M} , M_s is the full saturation of magnetization at $T=0$ K, and Ω is the correlation volume of anisotropy directions defined by

$$\Omega = \int_0^\infty 4\pi C(r)r^2 dr. \quad (6)$$

Magnetization measurements of powder samples of mass ~ 2 mg were carried out using a Faraday balance magnetometer¹ between 2.4 and 270 K at applied magnetic field up to 7.5 T. The correction for the demagnetization effect along the cylindrical axis was estimated to be too small to be considered within the accuracy of our field measurement. The low-field $M(H, T)$, $H < 5$ Oe, was measured using a Quantum Design MPMS2 superconducting quantum interference device (SQUID) magnetometer. Figure 1 shows the M vs T at various H . The T dependence of M is suppressed below $T_c \sim 140$ K compared with that of usual homogeneous ferromagnets, as usually observed for amorphous magnets. Measurements to H as high as 7.6 T at low T indicated a saturation magnetization in agreement with antiferromagnetic alignment V ($S = \frac{3}{2}$) and TCNE ($S = \frac{1}{2}$) spins resulting in a ferrimagnetic state.

In light of the disorder present in this compound, we compare the isothermal data at sufficiently low temperature (~ 4.5 K), Fig. 2(a), to the available RMA theory of Chudnovsky and co-workers developed at $T=0$ K for ferromagnets. Taking the derivative of Eq. (2), one has $M = M_s - 2^{1/3}B^{2/3}(dM/dH)^{1/3}$. The saturation magnetization M_s then can be estimated from the plot of M vs $(dM/dH)^{1/3}$. The intercept of the M axis with a straight

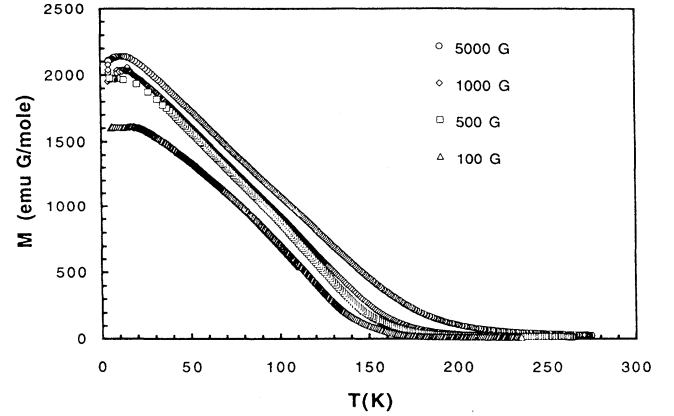


FIG. 1. M vs T of $V(TCNE)_{0.5}y(CH_3CN)$ at 5000, 1000, 500, and 100 Oe.

line extrapolated from the low-field data gives a value of $M_s = 5100 \sim 5500$ emu Oe/mol in reasonable agreement with the ferrimagnetic ordering noted above. Using Eq. (2), the constant anisotropy field H_c is determined by the intercept with the H axis from the plot of $(M_s - M)^{-2}$ vs H . By choosing $M_s = 5250$ emu Oe/mol to plot the data, we obtain $H_c = 21$ kOe and slope $B^{-2} = (4.8 \times 10^5$

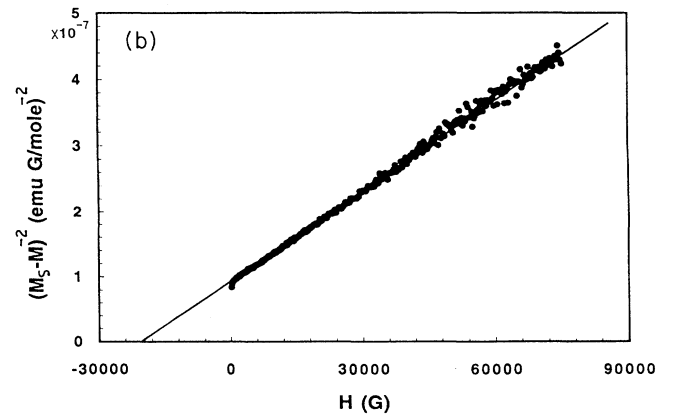
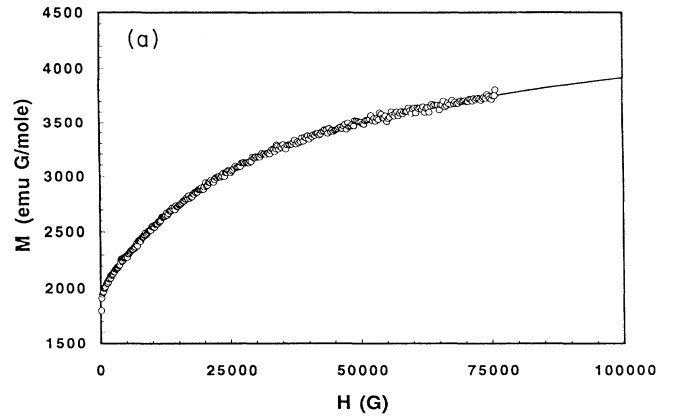


FIG. 2. (a) M vs H at $T = 4.4$ K. The solid line is the calculated results of Eq. (2); (b) $(M_s - M)^{-2}$ vs H with $M_s = 5250$ emu Oe/mol.

emu Oe^{3/2}/mol)⁻², Fig. 2(b). The agreement with Eq. (2) supports that the magnetic structure within this field regime is strongly noncollinear (FWA) with a characteristic tipping angle of spins $\theta \sim (H_r^4/H_{ex}^3 H)^{1/4}$, whose orientation may be locally preserved over length $R_\perp \ll H_{ex} R_a / 2H$.¹⁵ The field-cooled (< 3 G) and zero-field-cooled data show an irreversibility below $T_f = 10 \sim 14$ K varying with sample composition. We observed hysteresis effects below T_f (coercive field less than 10 G) and much less above T_f (coercive field < 1 G and a spontaneous $M < 1\%$ of the saturation M) suggesting a "reentrance" to a spin-glass state for T less than freezing temperature (T_f) at low H . Since the system is so soft, we suggest that this weak RMA system may be best described as a CSG for $H < (H_r^4/H_{ex}^3 - H_c)$ at $T > T_f$ with the characteristic that the local magnetization continuously rotates over the entire length of the sample, that is distance $\gg (H_{ex}/H_r)^2 R_a$ (long-range order is destroyed by local anisotropy).^{15,18,19} High-field ($H \sim H_{ex}$) $M(H)$ data are needed to obtain the short-range structural order correlation function $C(r)$ by the inverse Laplace transformation of Eq. (1).

Assuming typical exponential decay of correlation function $C(r) = e^{-r/R_a}$, Eq. (1) has the apparent field dependence^{15,16} $M_s - M = \Lambda^2 / 15p(1+p)^3$, where $p = [(H + H_c)/H_{ex}]^{1/2}$. Since H_{ex} is usually inaccessible, we could not obtain the value of H_{ex} from low-field data. For $p \rightarrow 0$ ($H \ll H_{ex}$), we have $M_s - M \rightarrow \Lambda^2 / 15p$. This is equivalent to Eq. (2) if in Eq. (4) one substitutes Ω/R_a^3 with 8π obtained by directly evaluating Eq. (6). With the value of B determined in Fig. 2, we obtain

$$\Lambda^2 H_{ex}^{1/2} \approx 7.2 \times 10^6 \text{ emu Oe}^{3/2}/\text{mol}. \quad (7)$$

In the FWA regime, although the correlation length is truncated to a limit

$$R_f = 60\pi M_s (R_a^3/\Omega) (R_a H_{ex}^{1/2}) / (\Lambda^2 H_{ex}^{1/2}),$$

it is still large ($R_f/R_a \gg 1$). With the known values of $\Lambda^2 H_{ex}^{1/2}$, M_s , and Ω/R_a^3 , we then have $H_{ex} \gg 3.3$ T, in agreement with the applicability of Eq. (2) to our field limit of ~ 8 T. We estimate $zJ \sim 280 \text{ K} \sim 380 \text{ T}$ from a mean-field expression for a simple ferromagnet with $T_c \simeq (2zJ/3k_B) S_e(S_e + 1)$ utilizing $T_c \simeq 140$ K and effective spin $S_e = \frac{1}{2}$. Using $R_a/a \sim 3$ from x-ray studies¹⁰ and Eq. (3), $H_{ex} \simeq 8.5$ T. Equation (7) then yields $\Lambda \simeq 160$ (emu Oe/mol)^{1/2}. Assuming $z = 6$ (octahedral structure) and knowing M_s , Λ , and R_a/a , Eq. (5) leads to $D_r/J \simeq 0.12$ or $D_r \simeq 5.5$ K. Since $H_c = 21 \text{ kG} \sim 2nD_c$, where n is the spin density of V^{++} , we have $D_c \sim 0.6$ K with $n \sim \frac{3}{2}$. Thus $J \gg D_r \gg D_c$ is consistent with the application of the RMA model.

We now address our isothermal results in the vicinity of T_c . We employ the equation of state and scaling law to analyze the isothermal data for $H < 6000$ Oe, Fig. 3(a). Plots of M^2 vs H/M (Arrott plots) show a large downward curvature away from linearity at low fields indicating that magnetization is suppressed. Indeed, the local magnetization fluctuation could be caused by both effects of random exchange and/or RMA. However, the large value of critical exponent $\beta \simeq 0.75$ obtained below T_c

(strong suppression of magnetization) compared with that for the usual quenched disorder systems with random exchange alone (< 0.5) (Ref. 20) supports the dominance of RMA. Since the distance between V and TCNE may vary little, the fluctuation in J may be less important than that in anisotropy. Correlated molecular-field theory showed that even for a strong exchange fluctuation case, the nonlinear behavior near T_c in the Arrott-Noakes plots would be minute, hence effective exponents should be close to the values of homogeneous critical exponents.^{21,22}

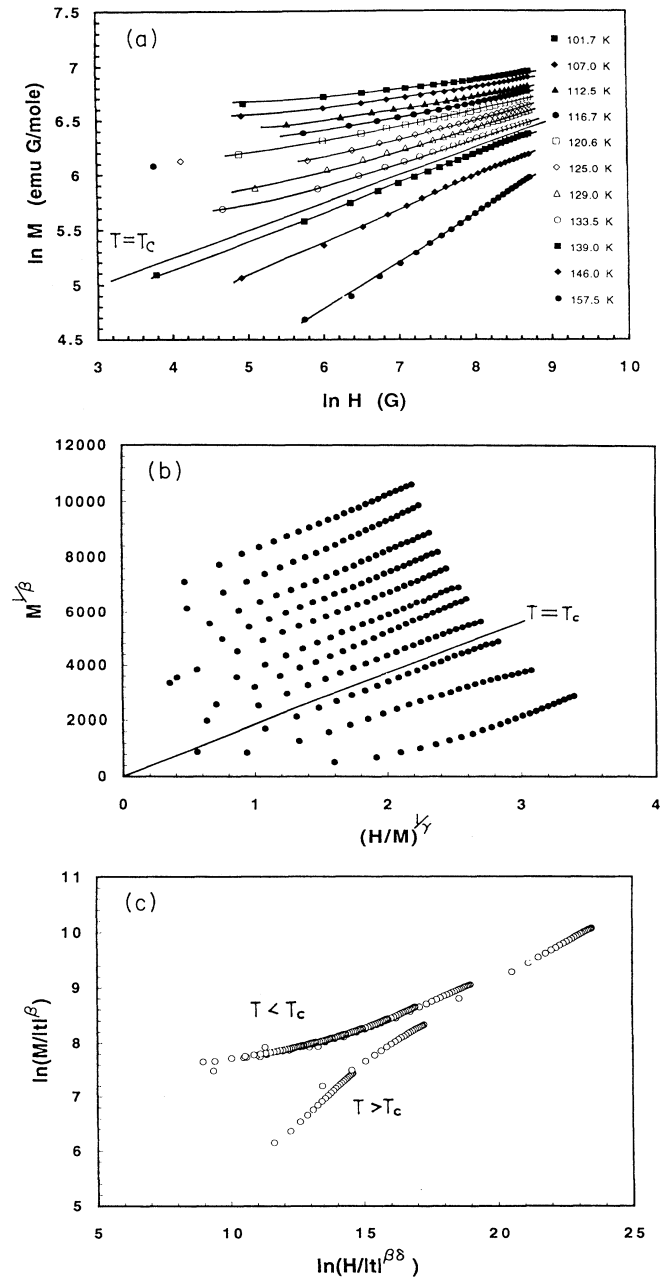


FIG. 3. (a) Isothermal M near T_c plotted as $\ln(M)$ vs $\ln(H)$. (b) The Arrott-Noakes plots with $\beta_a = 0.75$ and $\gamma_a = 2.25$ ($\delta_a = 4$); (c) scaling plot with $T_c = 138$ K (see text).

The inhomogeneity for the pure RMA case may be characterized by nonlinear leading terms, $\epsilon(D/J)$, in the equation of state that give rise to the RMA exponents for the isotherms as $\delta_a = (10-d)/(6-d)$ for $M \sim H^{1/\delta_a}$ ($T = T_c$) and $\delta_1 = (8-d)/(4-d)$ for $M \sim H^{1/\delta_1}$ ($T < T_c$), where d is the dimensionality.^{23,24} The critical exponent $\delta_a \simeq 4$ is estimated from the inverse slope of a straight line fit to the isothermal data in a logarithmic plot as closely as possible to T_c , Fig. 3(a). The exponent δ_1 cannot be experimentally identified here as we did not find a logarithmic behavior for all isotherms at $T < T_c$.

The Arrott-Noakes equation of state can be deduced if one replaces H/M with $(H/M)^{1/\gamma}$ and M^2 with $M^{1/\beta}$, that is $(H/M)^{1/\gamma} = t + aM^{1/\beta_a}$ with RMA critical exponent⁷ $\beta_a = (6-d)\beta/2$ and $t = (T - T_c)/T_c$. We note that $\beta_a = 0.75$ in the three-dimensional (3D) mean-field case ($\beta = 0.5$) appropriate for the 3D network structure of $V(\text{TCNE})_x \cdot y\text{CH}_3\text{CN}$. Figure 3(b) shows the results of the Arrott-Noakes plot with $\beta_a = 0.75$ and $\gamma_a = \beta_a(\delta_a - 1) = 2.25$ ($\delta_a = 4.0$). In principle, it is possible to obtain parallel isotherm lines by varying both values of β_a and δ_a . However, the true values of β_a and δ_a should simultaneously satisfy three conditions: (1) best parallel isotherm lines in the Arrott-Noakes plots, (2) a line passing through the origin corresponding to the critical isotherm ($T = T_c$), and (3) Widom's scaling relation $\gamma_a = \beta_a(\delta_a - 1)$. A systematic error could be present in the determination of δ_a owing to a difficulty of the measurement of the critical isotherm. Widom's relation can be verified by applying the general scaling form to analyze the isothermal data near T_c , $M/|t|^{\beta_a} = f(H/|t|^{\beta_a\delta_a}, t/|t|)$. $T_c = 138$ K was found due to the plot of scaled M vs scaled H with the "best" collapsing of the isothermal data into two branches for

$T < T_c$ and $T > T_c$, as shown in Fig. 3(c). As the three plots are consistent with each other, the values of the critical exponents for this RMA system with estimates of error are $\delta_a = 4.0 \pm 0.2$ and $\beta_a = 0.75 \pm 0.02$ for the sample shown. The relatively large value of β_a implies that effects of RMA dominate the inhomogeneous behavior near T_c . Although the value of δ_a is larger than that given by the 3D mean-field RMA theory ($\frac{7}{3}$), it is still smaller than that expected for most non-RMA systems. Thus the material has relatively strong field dependence of its critical isotherm compared to the non-RMA systems suggesting strong fluctuation of local magnetization due to the dominant effects of RMA.

In summary, magnetic studies of $V(\text{TCNE})_x \cdot y(\text{CH}_3\text{CN})$ provide strong support for the critical role of the spinless organic solvent in the disordered high- T_c molecular-based magnetic materials. We have shown that RMA concepts provide a quantitative description of the low temperature $M(H)$ and critical behavior near T_c . These results suggest that the critical feature governing the increase in T_c for the CH_2Cl_2 system is increased structural order yielding a reduced RMA. It is of interest to note that a detailed magnetic concept such as RMA previously applied to site-diluted and amorphous f and d electron systems⁷⁻⁹ can successfully account for magnetic phenomena in a molecular magnetic system for which a substantial fraction of the spin is supplied by p electrons and for which spinless organic solvent has a key role in determining magnetic properties.

We thank K. S. Narayan, K. R. Cromack, J. P. Pouget, S. M. Long, and M. S. Salamon for useful discussions and comments. This work was supported in part by DOE DMS Grant No. DE-FG-02-86BR45271.

*Present address: Dept. of Chem., Univ. of Utah, Salt Lake City, UT 84112.

¹S. Chittipeddi, K. R. Cromack, J. S. Miller, and A. J. Epstein, Phys. Rev. Lett. **58**, 2695 (1987).

²W. Broderick, J. Thompson, E. Day, and B. Hoffman, Science **249**, 401 (1990).

³G. T. Yee, J. M. Manriquez, D. A. Dixon, R. S. McLean, D. M. Gruski, R. B. Flippen, K. S. Narayan, A. J. Epstein, and J. S. Miller, Adv. Mater. **3**, 309 (1991).

⁴J. L. Paillaud, M. Drillon, A. de Cian, J. Fischer, R. Weiss, and G. Villeneuve, Phys. Rev. Lett. **67**, 244 (1991).

⁵M. Takahashi, P. Turek, Y. Nakazawa, M. Tamura, K. Nozawa, D. Shiomi, M. Ishikawa, and M. Kinoshita, Phys. Rev. Lett. **67**, 746 (1991).

⁶J. M. Manriquez, G. T. Yee, R. S. McLean, A. J. Epstein, and J. S. Miller, Science **252**, 1415 (1991).

⁷P. M. Gebring, M. B. Salamon, A. del Moral, and J. I. Arnaud, Phys. Rev. B **41**, 9134 (1990).

⁸J. Filippi, V. S. Amaral, and B. Barbara, Phys. Rev. B **44**, 2842 (1991).

⁹M. J. O'Shea, K. M. Lee, and A. Fert, J. Appl. Phys. **67**, 5769 (1990).

¹⁰Z. Oblakowski, J. P. Pouget, J. S. Miller, and A. J. Epstein (unpublished).

¹¹R. Crabtree, *The Organometallic Chemistry of the Transition*

Metals (Wiley, New York, 1988).

¹²J. S. Miller and A. J. Epstein, J. Am. Chem. Soc. **109**, 3850 (1987).

¹³A. L. Tchougreeff and R. Hoffmann, J. Phys. Chem. **97**, 350 (1993).

¹⁴E. M. Chudnovsky and R. A. Serota, Phys. Rev. B **26**, 2697 (1982); J. Phys. C **16**, 4181 (1983).

¹⁵E. M. Chudnovsky, W. M. Saslow, and R. A. Serota, Phys. Rev. B **33**, 251 (1986).

¹⁶E. M. Chudnovsky, Phys. Rev. B **33**, 2021 (1986); J. Magn. Magn. Mater. **64**, 5770 (1988); **79**, 127 (1989).

¹⁷V. Ignatchenko, R. Iskhakov, and G. Popov, Zh. Eksp. Teor. Fiz. **82**, 1518 (1982) [Sov. Phys. JETP **55**, 878 (1982)].

¹⁸Y. Imry and S. Ma, Phys. Rev. Lett. **35**, 1399 (1975).

¹⁹R. Pelcovits, E. Pytte, and J. Rudnick, Phys. Rev. Lett. **40**, 476 (1978).

²⁰S. N. Kaul, J. Magn. Magn. Mater. **53**, 5 (1985).

²¹M. Fahnle, G. Herzer, H. Kronmüller, R. Meyer, and M. Saile, J. Magn. Magn. Mater. **38**, 240 (1983); M. Fahnle and G. Herzer, *ibid.* **44**, 274 (1984).

²²M. Fahnle and M. Haug, Phys. Status Solidi B **140**, 569 (1987).

²³A. Aharony and E. Pytte, Phys. Rev. Lett. **45**, 1583 (1980); Phys. Rev. B **27**, 5872 (1983).

²⁴Y. Goldschmidt and A. Aharony, Phys. Rev. B **32**, 264 (1985).